Morphogeometric analysis for characterization of keratoconus considering the spatial localization and projection of apex and minimum corneal thickness point

Jose S. Velázquez [a], Francisco Cavas [a,*], David P. Piñero [b], Francisco J.F. Cañavate [a], Jorge Alio del Barrio [c,d,e], Jorge L. Alio [c,d,e]

[a] Department of Structures, Construction and Graphical Expression, Technical University of Cartagena, 30202 Cartagena, Spain
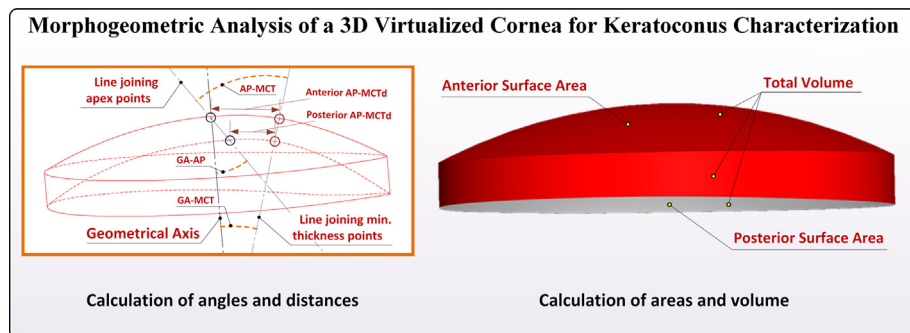[b] Group of Optics and Visual Perception, Department of Optics, Pharmacology and Anatomy, University of Alicante, 03690 Alicante, Spain
[c] Division of Ophthalmology, Miguel Hernández University, 03690 Alicante, Spain
[d] Keratoconus Unit of Vissum Corporation Alicante, 03690 Alicante, Spain
[e] Department of Refractive Surgery, Vissum Corporation Alicante, 03690 Alicante, Spain

GRAPHICAL ABSTRACT

Morphogeometric Analysis of a 3D Virtualized Cornea for Keratoconus Characterization

Calculation of angles and distances — Calculation of areas and volume

ARTICLE INFO

ABSTRACT

This work evaluates changes in new morphogeometric indices developed considering the position of anterior and posterior corneal apex and minimum corneal thickness (MCT) point in keratoconus. This prospective comparative study included 440 eyes of 440 patients (age, 7–99 years): control (124 eyes) and keratoconus (KC) groups (316 eyes). Tomographic information (Sirius®, Costruzione Strumenti Oftalmici, Italy) was treated with SolidWorks v2013, creating the following morphogeometric parameters: geometric axis–apex line angle (GA–AP), geometric axis–MCT line angle (GA–MCT, apex line–MCT line angle (AP–MCT), and distances between apex and MCT points on the anterior (anterior AP–MCTd) and posterior corneal surface (posterior AP–MCTd). Statistically significant higher values of GA–AP, GA–MCT, AP–MCT and anterior AP–MCTd were found in the keratoconus group ($p \leq 0.001$). Moderate significant correlations of corneal aberrations ($r \geq 0.587$, $p < 0.001$) and corneal thickness parameters ($r \leq -0.414$, $p < 0.001$) with GA–AP and AP–MCT were found. Anterior asphericity was found to be significantly correlated with anterior and posterior AP–MCTd ($r \geq 0.430$, $p < 0.001$). Likewise, GA–AP and AP–MCT showed a good diagnostic ability for the detection of keratoconus, with optimal cutoff values

of 9.61° (sensitivity 85.5%, specificity 80.3%) and 18.08° (sensitivity 80.5%, specificity 78.7%), respectively. These new morphogeometric indices allow a clinical characterization of the 3-D structural alteration occurring in keratoconus, with less coincidence in the spatial projection of the apex and MCT points of both corneal surfaces. Future studies should confirm the potential impact on the precision of these indices of the variability of posterior corneal surface measurements obtained with Scheimpflug imaging technology.

Introduction

The morphogeometric analysis of the corneal structure has been shown to be a valuable tool to characterize the keratoconic cornea, allowing a better understanding of the macrostructural consequences of the degenerative process associated to this disease [1]. This is especially useful for the generation of new indices, which allows for sensitive and specific detection of keratoconus (KC), even in the most incipient stages [2,3]. It should be taken into account that the analysis of the geometry of the anterior corneal surface is insufficient for the detection of subclinical or incipient KC; therefore, it is necessary to consider other additional descriptors, such as corneal asphericity and aberrations, pachymetry, or corneal biomechanics [4–10].

The analysis of corneal symmetry has been also evaluated as a potential tool to ease the detection of incipient ectatic stages, especially in terms of decentration of the apex position [11–14]. Wahba et al [11] found that one of the parameters showing the highest diagnostic ability for early keratoconus compared to normal corneas was the diagonal de-centration of the thinnest point from the apex. Abu Ameerh et al. [12], in a study evaluating a sample of Jordanian patients, found that the vertical pachymetric apex position had a good correlation with KC severity grades, while the horizontal position seemed to remain unaffected. Likewise, Fredriksson and Behndig [13] confirmed that many astigmatic values in keratoconus differed between the 3 mm pupil-centred and the 3 and 6 mm apex-centred zones. In the current study, a new approach based on corneal morphogeometric analysis considering the symmetry of vertex position and the point of minimum corneal thickness (MCT) has been proposed and evaluated. Specifically, the focus of this research was to evaluate changes occurring in these new morphogeometric indices with consideration of the position of anterior and posterior corneal apices and the MCT point in keratoconus and the correlation of these changes according to the severity of the disease.

Material and methods

Patients

This prospective comparative study enrolled 440 eyes from 440 patients with ages varying from 7 to 99 years old. A random selection of just one eye from each subject was made to elude the potential bias associated to the correlation between both eyes of the same individual. The study was supervised at the Keratoconus Unit of Vissum Corporation Alicante, Spain, (a center affiliated with Miguel Hernández University of Elche, Spain) and was ratified by the Ethics Commission of this institution following ethical standards of the Declaration of Helsinki (7th revision, October 2013, Fortaleza, Brazil). The sample, which is part of the official database "Iberia" of keratoconus cases created for the National Network for Clinical Research In Ophthalmology RETICS-OFATARED, was divided into two groups: a control one, that included 124 healthy eyes, and a KC other, composed of 316 eyes diagnosed with KC.

Inclusion criteria were the presence of a healthy eye—not meeting the exclusion criteria for the control group—and a KC diagnosis according to the standard criteria for the KC group [15,16]. These criteria are based on the presence of the following signs: anterior corneal topographic asymmetric bowtie pattern, KISA ≥ 100, and one or more biomicroscopic keratoconus signs, such as Fleischer ring, significant corneal thinning, Vogt striae or conical protrusion on the cornea at the apex. Previous ocular surgery, presence of opacities and/or any other active ocular disease were considered as exclusion criteria. Keratoconus eyes with previous corneal surgeries, such as corneal collagen crosslinking or intrastromal ring segment insertion, were excluded from the KC group.

Examination protocol

A thorough clinical eye examination was conducted in all subjects including measurement of uncorrected (UDVA) and corrected distance visual acuity (CDVA), anamnesis, objective and subjective refraction, slit-lamp biomicroscopy, and corneal analysis with the Sirius topographic system (Costruzione Strumenti Oftalmici, Italy). All tests were performed by a single experienced examiner. A minimum of three corneal topographies were successively obtained for each cornea and the best one (the topography with the highest acquisition quality for the Scheimpflug image and keratoscopy) was selected to provide data for this study. According to this exam, each keratoconus case was graded in terms of severity using the Amsler–Krumeich grading system [17]. Besides this, all corneal tomographic files were exported in .csv format to be analyzed in detail using a morphogeometric analysis procedure developed and endorsed by our research group [1–3].

Morphogeometric analysis

The method of morphogeometric examination used in this research work was based on the following steps (Fig. 1):

1. Generation of the point cloud. A coordinate system for a three-dimensional space was used to generate the surface according to the point cloud data. Exported CSV tomographic files from Sirius tomographer provide spatial points that conform to corneal surfaces, coordinates of each scanned point are given in polar format (radii and semi-meridians), and some scanned points can present a reading error caused by extrinsic factors [18], so an algorithm programmed using Matlab® V R2014 (Mathworks, Natick, USA) software was developed to: i) obtain the Cartesian format of the polar coordinates included in each topography file, and ii) eliminating the topograhy files that contain invalid reading data in polar coordinates (value = − 1000). Regarding the CSV topography files from Sirius tomographer, every row was considered a representation of a circle in the corneal map, with every column representing a semi-meridian (256 points per radius). Each row represents a sample taken following the plot of a circle of radius i*0.2 mm, with "i" being the number of the row, and each column represents a sample taken following the plot of a semimeridian in the direction of
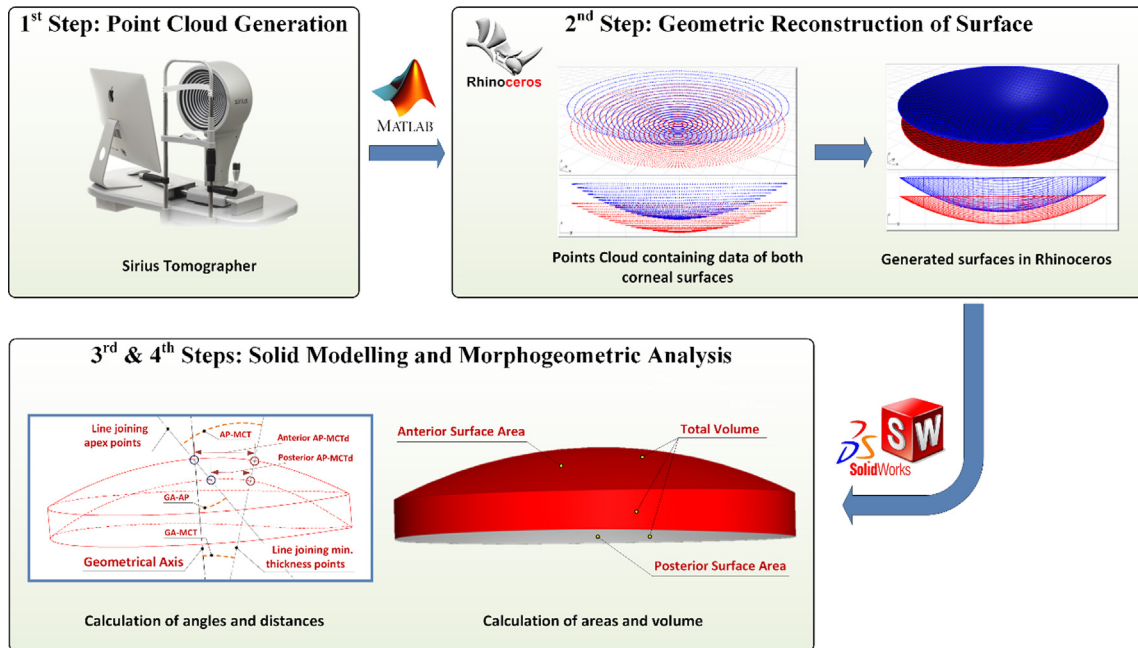
Fig. 1. Scheme of the procedure for the generation of a virtual corneal model and morphogeometrical variables definition, based on angular–spatial relations. GA–AP: Geometrical axis–apex line angle; GA–MCT: Geometrical axis–minimum thickness line angle; AP–MCT: Apex line–minimum thickness line angle; Anterior/Posterior AP–MCTd: Distance between apex and minimal corneal thickness points on the anterior/posterior corneal surface.

j*360/256u, with "j" being the number of the column. Finally, an [i, j] matrix was generated, in which each Z value represents the point P (i*0.2, j*360/256u) in polar coordinates. With this organization, a cloud of points was generated specifically for a zone extending from the normal corneal vertex (corneal geometric centre, r = =0 mm) to the mid-peripheral zone (r = =4 mm), this criterion is mainly justified by the following two reasons: Geometric principle [1,2] and Clinical principle [19], as this zone of analysis tends to include most information on corneal morphology, not only for healthy but also for diseased eyes.

2. Geometric rebuild of corneal surface. An importation of the cloud of points representative of the corneal architecture into the surface reconstruction software Rhinoceros® V 5.0 (MCNeel & Associates, Seattle, USA) was performed. This software uses a mathematical model to generate surfaces based on non-uniform rational B-splines (NURBS) [20], and its validity in the Biomedical Engineering field [21–24] and the Ophthalmology field [2,3,25–28] has been widely demonstrated, as when these functions are based on a dense and uniform distribution of scanned sample points, they bestow the geometric fidelity of the original surface upon the new structure. In our study, the Rhinoceros's patch surface function was selected to find the surface best fitting the cloud of points, with a minimization of the nominal separation between the three-dimensional cloud of points and the generated surface. This deviation can be later calculated by the software, providing a mean value of the distance error for the solution surface [25]. The following configuration settings were used for the function: sample point spacing 256, surface span planes 255 for both u and v directions, and stiffness of the solution surface [1].

3. Solid Modelling. The surface obtained in the previous step was then imported into the solid modelling software SolidWorks® V 2012 (Dassault Systèmes, Vélizy-Villacoublay, France). Using this software, the custom model that represents the corneal geometry was created [1].

4. Calculation of different morphogeometric parameters from the solid model generated. Some of these variables have been defined in detail in previous studies of our research group [1–3]: anterior corneal surface (ACS) area (A_{ant}), posterior corneal surface (PCS) area (A_{post}), total corneal surface area (A_{tot}), and corneal volume (CV). Regarding the areas, the measured area comprises the corneal surface for a radius = 4 mm from its normal corneal vertex, which included the central and paracentral regions [18]. Regarding the geometrical axis [29], given that the cornea does not have a perfect symmetry axis, and that the optical axis is not real, the, geometrical axis is defined as the centreline that can be used as a reference in modelling applications in computer-aided design (CAD) or finite element (FE) modelling packages, and is calculated as an axis normal to the tangent plane in the geometric centre (vertex). Likewise, the following new morphogeometric variables were defined for healthy (Fig. 2) and advanced keratoconus eyes (Fig. 3):

- Geometrical axis–apex line angle (GA–AP): angle between the optic axis and the line joining the apex points of ACS and PCS.
- Geometrical axis–minimum thickness line angle (GA–MCT): angle between the optic axis and the line joining the points of the ACS and PCS in the corneal section containing the minimum corneal thickness.
- Apex line–minimum thickness line angle (AP–MCT): angle between the line joining the apex points of the ACS and PCS and the line joining the points of the ACS and PCS in the corneal section containing the minimum corneal thickness.
- Distance between apex and minimal corneal thickness points on the ACS (Anterior AP–MCTd): length of the segment joining the apex and point and minimum thickness point on the ACS.
- Distance between apex and minimal corneal thickness points on the PCS (Posterior AP–MCTd): length of the segment joining the apex and point and minimum thickness point on the PCS.
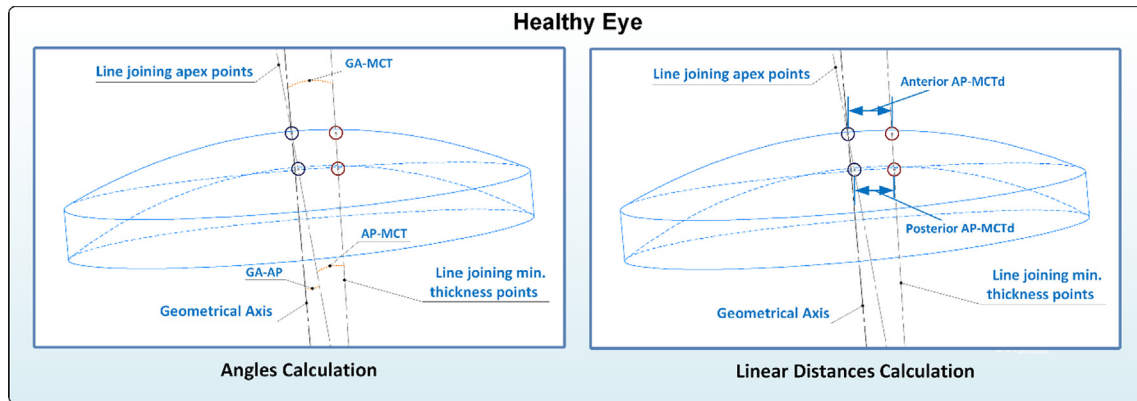
Fig. 2. Graphical representation of angles and linear distances calculation for a healthy eye (male patient of 31 years, OD, CDVA = 1, astigmatism = 1.18, comma-like = 0.43, spherical-like = 0.16, Q_{8mm} = − 0.51 central thickness = 483), GA–AP = 6.48°, GA–MCT = 6.57°, AP–MCT = 12.95°, Anterior AP–MCTd = 0.604 mm, Posterior AP–MCTd = 0.495 mm). GA–AP: Geometrical axis–apex line angle; GA–MCT: Geometrical axis–minimum thickness line angle; AP–MCT: Apex line–minimum thickness line angle; Anterior/Posterior AP–MCTd: Distance between apex and minimal corneal thickness points on the anterior/posterior corneal surface.
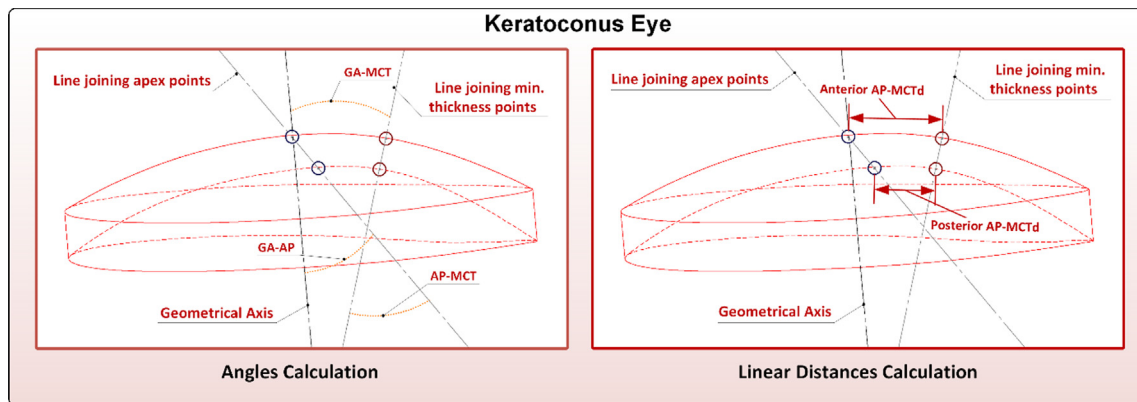
Fig. 3. Graphical representation of angles and linear distances calculation for an advanced keratoconus eye (male patient of 20 years, OD, CDVA = 0.44, astigmatism = 1.77, comma-like = 2.27, spherical-like = 2.50, Q_{8mm} = − 2.42 central thickness = 447), GA–AP = 9.08°, GA–MCT = 11.04°, AP–MCT = 18.16°, Anterior AP–MCTd = 1.159 mm, Posterior AP–MCTd = 0.796 mm). GA–AP: Geometrical axis–apex line angle; GA–MCT: Geometrical axis–minimum thickness line angle; AP–MCT: Apex line–minimum thickness line angle; Anterior/Posterior AP–MCTd: Distance between apex and minimal corneal thickness points on the anterior/posterior corneal surface.

Statistical analysis

The SPSS statistics software package, version 15.0 (IBM, Armonk, EEUU), was the one chosen to perform the statistical analysis of data. The normality of all data was checked by means of a Kolmogorov–Smirnov test. The unpaired Student's *t*-test was used to assess the statistical significance of differences between control and keratoconus groups. Furthermore, the correlation between anterior and posterior geometric parameters was assessed with the calculation of the Pearson correlation coefficient. All differences for which the related p-value was < 0.05 were considered statistically significant.

The intrasubject repeatability for the pachymetrical parameters CCT and MTC was assessed by using the following statistical variables: the within-subject standard deviation (S_w) of the consecutive measurements (three in total), intrasubject repeatability (IR), the coefficient of variation (CoV), and the intraclass correlation coefficient (ICC). The Sw is an easy way of estimating the magnitude of the measurement error. The intraobserver precision was as ± 1.96 × S_w, giving this value an estimation on the size of the error of the consecutive measures for 95% of the observations. The ICC is a correlation based in the analysis of variance (ANOVA) that measures the relative homogeneity within groups (for the set of repeated measurements) with regards to the total variation. The ICC will tend to 1.0 when the variance within the repeated measures tend to zero, indicating that the total variation in measurements can only be attributed to variability in the measured parameter.

The spherocylindrical refraction in each case was converted to vectorial notation using the power vector method of Thibos and Horner [30]. With this method, all spherocylindrical refractive errors in conventional script notation (S [sphere], C [cylinder] × φ [axis]) could be converted to power vector coordinates and overall blurring strength (B) using the following formulae: M = S + C/2; J_0 = (−C/2) cos (2 φ); J_{45} = (−C/2) sin (2 φ); and B = $(M^2 + J_0^2 + J_{45}^2)^{1/2}$.

Finally, the diagnostic ability of the parameters defined from the morphogeometric analysis performed to detect keratoconus was evaluated using the receiver operating characteristic (ROC) curve analysis for half of the population evaluated. This subgroup of eyes was selected randomly. ROC curves show the relationship between sensitivity (pathological cases that are correctly detected) and 1-specificity (non-pathological cases that have a negative test result). Furthermore, this analysis provides the area under the curve and its corresponding statistical significance, which allows the clinician to determine the diagnostic accuracy of any clinical parameter evaluated. Likewise, an optimal cutoff is defined, which corresponds to the point of the curve which has high sensitivity while maintaining a high specificity (compromise between sensitivity and specificity). In the current study, once obtained the

ROC curve, its diagnostic ability for the detection of keratoconus was validated with the other half of the sample not included in the previous analysis, detecting the percentage of true positives (TP) and negatives (TN). Specifically, false positive (FP) and false negative (FN) rates were calculated as well as positive (PPV = TP/(TP + FP)) and negative predictive values (NPV = TN/(TN + FN)).

Results

A total amount of 124 healthy eyes from 124 subjects (28.2%) (control group, C) and 316 keratoconus eyes from 316 subjects (71.8%) (keratoconus group, KC) were considered in the study. The mean age of the sample was 38.4 years (standard deviation, SD: 15.6; median: 36.0; range: 7 to 99 years). According to the Amsler–Krumeich grading system, the severity of the disease was distributed as follows in the analyzed sample: 223 eyes with grade I (70.6%), 57 eyes with grade II (57 eyes), 9 eyes with grade III (2.8%), and 27 eyes with grade IV (8.5%). The main clinical characteristics in the control and KC group are summarized in Table 1. As shown, statistically significant differences were found between groups in refraction, CDVA, anterior and posterior corneal asphericity, corneal higher-order aberrations and pachymetry ($p \leq 0.001$).

Table 2 shows the intrasubject repeatability results for the pachymetrical variables analyzed with the Sirius system. An S_w value below 4 µm was observed for the pachymetry measurements for both the control and keratoconus groups, with ICC values close to 1 and a CoV below 0.7% in all cases. No significant differences were found in the S_w values associated with the minimum and central pachymetry measurements (p = 0.47).

Table 3 summarizes the outcomes obtained in the morphogeometric analysis in control and KC groups. Statistically significant higher values of A_{ant} and A_{post} were obtained in the KC group compared to the control group (p < 0.001). Likewise, statistically significant higher values of corneal volume were found in the keratoconus group (p < 0.001). Concerning the new morphogeometric parameters, statistically significant higher values of GA–AP, GA–MCT, AP–MCT and anterior AP–MCTd were also found in the KC group compared to the control group ($p \leq 0.001$).

In the control group, very weak correlations were found between the new morphogeometric parameters and other clinical parameters measured ($-0.209 \leq r \leq 0.246$, $p \geq 0.006$). In contrast, in the KC group, several significant correlations were found, as summarized in Table 4. Moderate significant correlations of corneal aberrations ($r \geq 0.587$, p < 0.001), especially coma RMS (Figs. 4 and 5), and corneal thickness parameters ($r \leq -0.414$, p < 0.001) with GA–AP and AP–MCT were found. Anterior Q for 4.5-mm and 8-mm areas were found to be significantly correlated with anterior AP–MCTd ($r \geq 0.430$, p < 0.001) (Fig. 6) and posterior AP–MCTd ($r \geq 0.550$, p < 0.001) (Fig. 7). Finally, the correlations of keratoconus grade severity with the morphogeometric parameters evaluated were more limited ($-0.225 \leq r \leq 0.418$, p < 0.001).

Concerning the ROC curve analysis, with half of the population evaluated, GA–AP and AP–MCT had the best diagnostic ability for the detection of keratoconus, with areas under the curve (AUC) of 0.908 and 0.891, respectively (p < 0.001). The optimal cutoff values for these parameters were 9.61° (sensitivity 85.5%, specificity 80.3%) and 18.08° (sensitivity 80.5%, specificity 78.7%), respectively. For the rest of the morphogeometric parameters, the AUC ranged from 0.682 (p < 0.001) for GA–MCT to 0.543 (p = 0.320)

Table 1
Summary of the visual acuity, refractive, pachymetric, and corneal topographic and aberrometric data obtained in control and keratoconus groups. The statistical significance (p-value) of the difference between these two groups for each parameter evaluated is displayed. Abbreviations: SD, standard deviation; D, diopter; SE, spherical equivalent; J_0 and J_{45}, astigmatic power vector components; B, overall blur strength; CDVA, corrected distance visual acuity; Q, asphericity; HOA, higher-order aberrations; RMS, root mean square; SA, spherical aberration; CCT, central corneal thickness; MCT, minimum corneal thickness.

Mean (SD) Median (Range)	Control	Keratoconus	p-value
Sphere (D)	−0.64 (3.62) 0.00 (−12.50 to 8.00)	−2.43 (4.47) −1.00 (−20.00 to 5.00)	<0.001
Cylinder (D)	−0.62 (0.75) −0.50 (−5.75 to 0.00)	−2.80 (2.37) −2.25 (−17.00 to 0.00)	<0.001
SE (D)	−0.95 (3.61) 0.00 (−12.88 to 8.12)	−3.83 (4.62) −2.38 (−21.75 to 4.00)	<0.001
J_0 (D)	0.12 (0.41) 0.00 (−0.59 to 2.70)	−0.21 (1.24) −0.17 (−4.25 to 5.00)	<0.001
J_{45} (D)	−0.01 (0.23) 0.00 (−0.98 to 1.37)	0.15 (1.33) 0.00 (−4.00 to 7.36)	0.139
B (D)	2.65 (2.66) 1.93 (0.00 to 12.88)	4.53 (4.34) 3.02 (0.00 to 21.82)	<0.001
LogMAR CDVA	0.00 (0.04) 0.00 (−0.08 to 0.22)	0.20 (0.28) 0.10 (−0.18 to 1.30)	<0.001
Anterior Q 4.5 mm	−0.09 (0.27) −0.07 (−0.65 to 0.84)	−0.60 (1.54) −0.59 (−7.42 to 4.10)	0.001
Anterior Q 8.0 mm	−0.25 (0.19) −0.25 (−0.78 to 0.13)	−0.88 (0.84) −0.76 (−3.00 to 2.82)	<0.001
HOA RMS (µm)	0.42 (0.11) 0.40 (0.24 to 0.76)	2.91 (2.37) 2.31 (0.32 to 13.84)	<0.001
Coma RMS (µm)	0.28 (0.12) 0.26 (0.02 to 0.61)	2.36 (2.12) 1.88 (0.04 to 12.85)	<0.001
SA (µm)	0.22 (0.06) 0.22 (0.08 to 0.42)	−0.30 (1.19) 0.11 (−7.85 to 1.32)	<0.001
Spherical-like RMS (µm)	0.24 (0.06) 0.24 (0.11 to 0.48)	1.05 (1.15) 0.67 (0.15 to 8.29)	<0.001
Coma-like RMS (µm)	0.33 (0.13) 0.32 (0.08 to 0.70)	2.62 (2.16) 2.19 (0.20 to 12.95)	<0.001
CCT (µm)	544.33 (32.27) 544.50 (482 to 639)	468.38 (59.82) 475.00 (285 to 633)	<0.001
MCT (µm)	541.09 (32.03) 541.00 (480 to 634)	449.56 (66.09) 455.00 (231 to 602)	<0.001

Table 2
Intrasubject repeatability results for the pachymetrical variables analyzed with the Sirius system. Abbreviations: SD, standard deviation; CCT, central corneal thickness; MCT, minimum corneal thickness; S_w: within-subject standard deviation; CoV: coefficient of variation; IR: intrasubject repeatability; ICC: intraclass correlation coefficient; CI: confidence interval.

	Variables	Mean (SD) Median (Range)	S_w	CoV (%)	IR	ICC	Range 95% CI
Control	CCT (μm)	544.33 (32.27) 544.50 (482 to 639)	2.79	0.51	5.50	0.996	0.995, 0.997
	MCT (μm)	541.09 (32.03) 541.00 (480 to 634)	2.81	0.51	5.51	0.996	0.995, 0.997
Keratoconus	CCT (μm)	468.38 (59.82) 475.00 (285 to 633)	2.29	0.49	4.48	0.997	0.996, 0.998
	MCT (μm)	449.56 (66.09) 455.00 (231 to 602)	3.21	0.69	6.19	0.989	0.982, 0.994

Table 3
Summary of the different corneal parameters defined and obtained from the morphogeometric analysis performed in both control and keratoconus groups. The statistical significance (p-value) of the difference between these two groups for each parameter evaluated is displayed. Abbreviations: SD, standard deviation; A_{ant}, anterior corneal surface area; A_{post}, posterior corneal surface area; A_{tot}, total corneal surface area; CV, corneal volume; GA–AP, geometrical axis–apex line angle; GA–MCT, geometrical axis–minimum thickness line angle; AP–MCT, apex line–minimum thickness line angle; anterior AP–MCTd, distance between apex and minimum corneal thickness points on the anterior corneal surface; posterior AP–MCTd, distance between apex and minimum corneal thickness points on the posterior corneal surface.

Mean (SD) Median (Range)	Control	Keratoconus	p-value
A_{ant} (mm^2)	43.09 (0.15) 43.10 (42.73 to 43.39)	43.48 (0.55) 43.36 (42.49 to 47.44)	<0.001
A_{post} (mm^2)	44.26 (0.29) 44.26 (43.49 to 44.90)	44.87 (0.90) 44.69 (43.57 to 51.14)	<0.001
A_{tot} (mm^2)	104.01 (1.19) 103.93 (100.72 to 106.15)	104.15 (2.00) 103.81 (99.96 to 114.88)	0.622
CV (mm^3)	25.85 (1.49) 25.95 (22.99 to 29.50)	23.87 (1.82) 23.81 (16.95 to 28.96)	<0.001
GA–AP °	7.19 (2.20) 7.03 (2.49 to 13.33)	21.99 (11.15) 21.23 (1.32 to 67.26)	<0.001
GA–MCT °	8.26 (5.30) 7.59 (0.53 to 50.12)	9.76 (5.28) 9.05 (0.44 to 52.37)	<0.001
AP–MCT °	15.03 (6.02) 14.07 (4.15 to 56.68)	30.89 (13.12) 29.81 (0.15 to 75.19)	<0.001
Anterior AP–MCTd (mm)	0.87 (0.25) 0.84 (0.44 to 1.98)	1.02 (0.40) 0.96 (0.17 to 3.20)	0.001
Posterior AP–MCTd (mm)	0.74 (0.24) 0.71 (0.34 to 2.20)	0.76 (0.37) 0.71 (0.05 to 2.86)	0.722

Table 4
Summary of the different statistically significant correlations found between corneal parameters defined and obtained from the morphogeometric analysis and different clinical data in the keratoconus group. The statistical significance (p-value) of correlations is also displayed. Abbreviations: SD, standard deviation; A_{ant}, anterior corneal surface area; A_{post}, posterior corneal surface area; A_{tot}, total corneal surface area; CV, corneal volume; GA–AP, geometrical axis–apex line angle; GA–MCT, geometrical axis–minimum thickness line angle; AP–MCT, apex line–minimum thickness line angle; anterior AP–MCTd, distance between apex and minimum corneal thickness points on the anterior corneal surface; posterior AP–MCTd, distance between apex and minimum corneal thickness points on the posterior corneal surface; CDVA, corrected distance visual acuity; Q, asphericity; HOA, higher-order aberrations; RMS, root mean square; SA, spherical aberration; CCT, central corneal thickness; MCT, minimum corneal thickness.

| Morphogeometric parameters	Correlated with	Correlation coefficient	p-value
GA–AP °	CDVA	0.428	<0.001
	HO RMS	0.753	<0.001
	Coma RMS	0.75	<0.001
	Coma-like RMS	0.749	<0.001
	Spherical-like RMS	0.655	<0.001
	Anterior Q in central 8 mm	−0.487	<0.001
	KC grade severity	0.418	<0.001
	MCT	−0.618	<0.001
	CCT	−0.486	<0.001
GA–MCT °	KC grade severity	0.155	0.006
AP–MCT °	HO RMS	0.667	<0.001
	Coma RMS	0.664	<0.001
	Coma-like RMS	0.662	<0.001
	Spherical-like RMS	0.587	<0.001
	KC grade severity	0.367	<0.001
	MCT	−0.55	<0.001
	CCT	−0.414	<0.001
Anterior AP–MCTd (mm)	Anterior Q in central 4.5 mm	0.6	<0.001
	Anterior Q in central 8 mm	0.43	<0.001
	KC grade severity	−0.18	0.001
Posterior AP–MCTd (mm)	Anterior Q in central 4.5 mm	0.65	<0.001
	Anterior Q in central 8 mm	0.55	<0.001
	KC grade severity	−0.225	<0.001
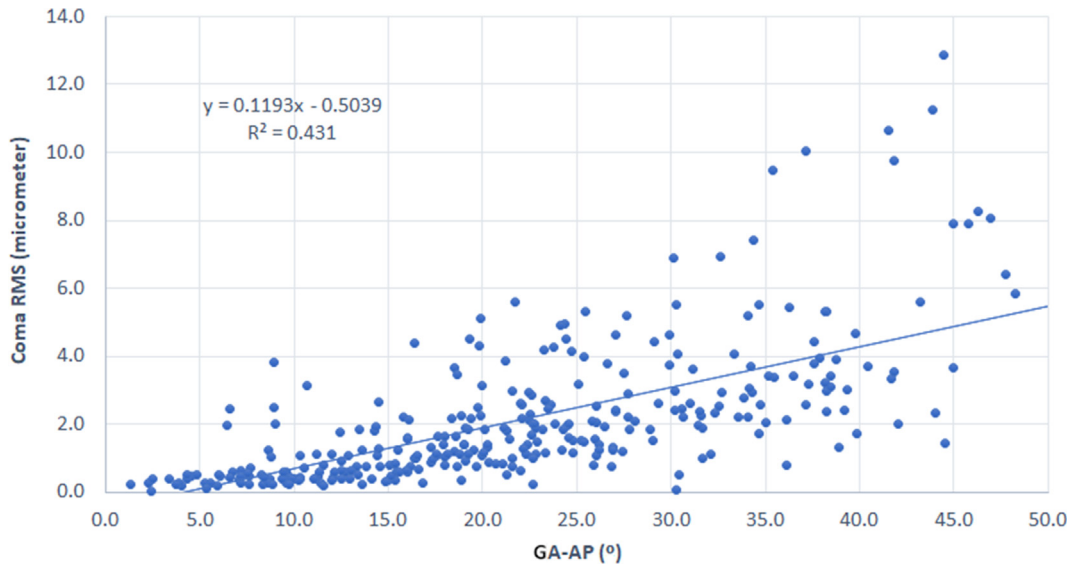
Fig. 4. Scatterplot showing the relationship between the geometrical axis–apex line angle (GA–AP) defined from the morphogeometric analysis performed and the level of corneal primary coma aberration in terms of the root mean square (RMS) obtained in the keratoconus group. The adjusting line to the data obtained by means of the least-squares fit is shown.
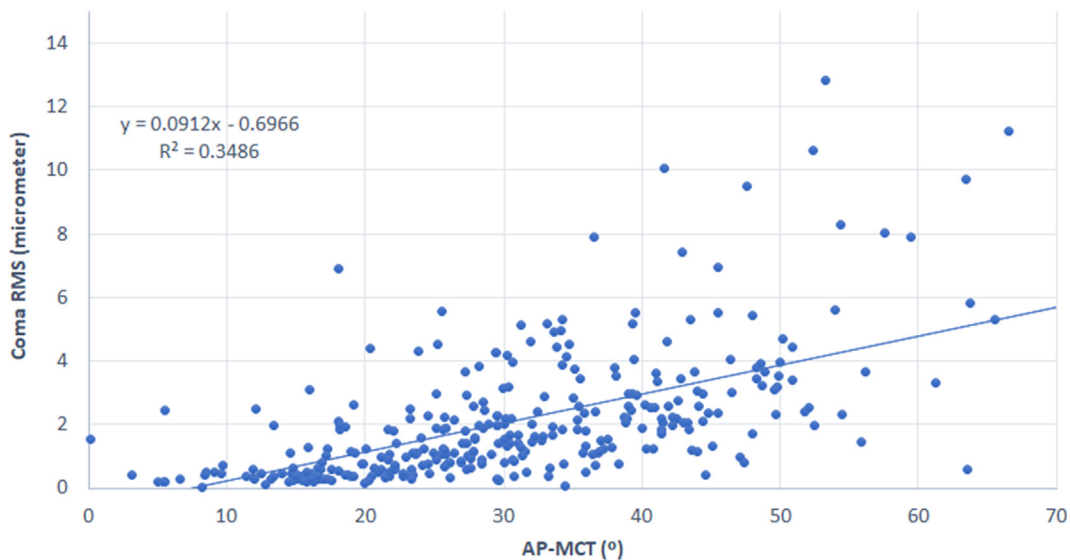

Fig. 5. Scatterplot showing the relationship between the apex line–minimum thickness line angle (AP–MCT) defined from the morphogeometric analysis performed and the level of primary coma aberration in terms of root mean square (RMS) obtained in the keratoconus group. The adjusting line to the data obtained by means of the least-squares fit is shown.

for posterior AP–MCTd. When the cutoff point obtained for GA-AP was validated with the other half of the sample, FP and FN rates of 9.7% and 15.2% were found, respectively. Likewise, PPV and NPV of 95.8% and 71.8% were obtained, respectively. Considering the cut-off point obtained for AP-MCT, FP, FN, PPV, and NPV values of 24.2%, 15.2%, 89.9%, and 66.2%, respectively.

Discussion

Several technological advances have been introduced in clinical practice to characterize and evaluate in detail the corneal changes occurring in keratoconus [15,31]. Besides a great variety of tools for early detection of keratoconus [15,31], even considering the cornea as a solid with a determined volume [2,3], different tomographic, pachymetric, optical and biomechanical indices have been devel-

oped to characterize the level of severity of the disease and to monitor the potential progression of the structural weakening of the cornea [11,12,17,31–39]. In the current study, we have used a Scheimpflug imaging-based tomographer that have been previously validated, the Sirius system, which can provide repeatable geometric and pachymetric measurements in healthy [40–43] and keratoconus eyes [44,45]. Likewise, previous comparative clinical studies have demonstrated the good interchangeability level of pachymetric measurements obtained with the Sirius system and anterior segment optical coherence tomography systems [46–48]. The variability of repeated measurements of pachymetry parameters evaluated in the current study was below 4 μm, which is not clinically relevant, and coincides with the results of previous studies [43,44].

Regarding the geometric calculations performed with the data obtained with the tomographer used, we have considered the
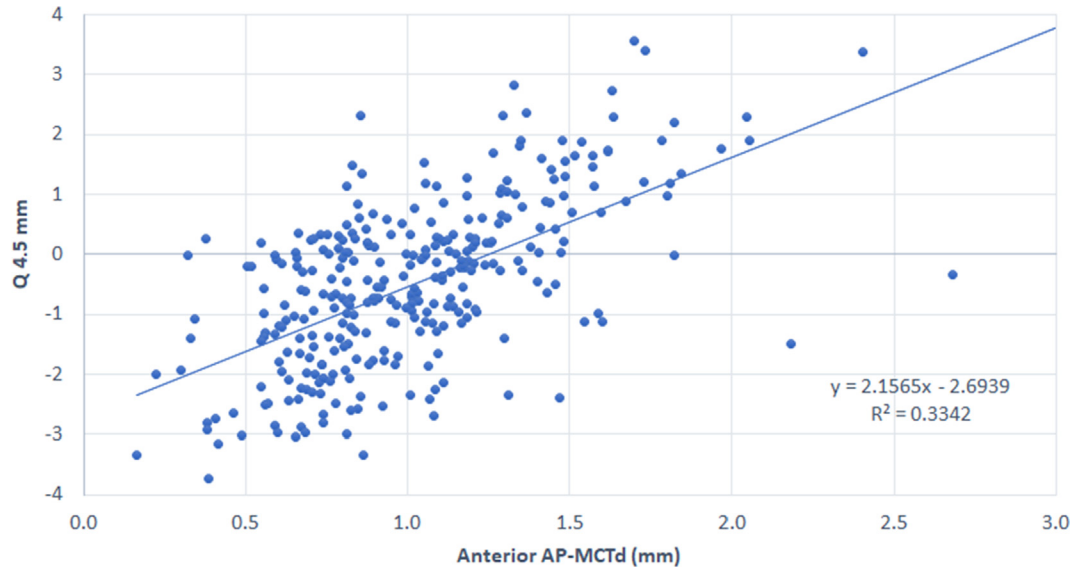
Fig. 6. Scatterplot showing the relationship between the distance between apex and minimum corneal thickness points on the anterior corneal surface (Anterior AP–MCTd) defined from the morphogeometric analysis performed and the anterior corneal asphericity (Q) in the central 4.5 mm area obtained in the keratoconus group. The adjusting line to the data obtained by means of the least-squares fit is shown.

Fig. 7. Scatterplot showing the relationship between the distance between apex and minimum corneal thickness points on the posterior corneal surface (Anterior AP–MCTd) defined from the morphogeometric analysis performed and the anterior corneal asphericity (Q) in the central 4.5 mm area obtained in the keratoconus group. The adjusting line to the data obtained by means of the least-squares fit is shown.
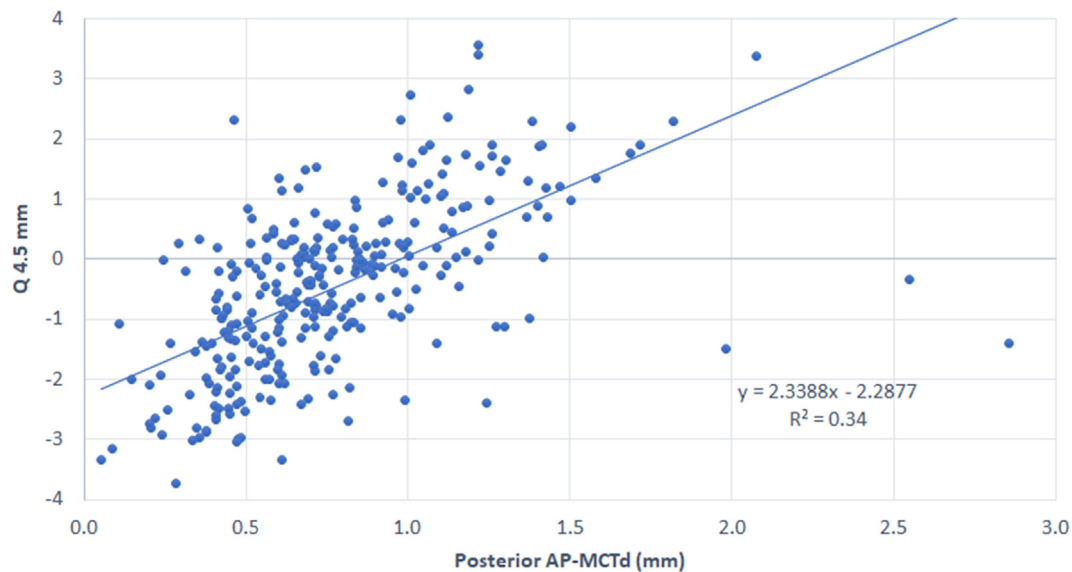
cornea as a solid, with the definition of new morphogeometric parameters by means of a new mathematical approach [1] in order to characterize potential changes in the symmetric distribution of some reference points on the two surfaces of the cornea. Specifically, the geometrical axis (GA), the line joining the apex points of the ACS and PCS (AP), and the line joining the points of the ACS and PCS in the corneal section containing the minimum corneal thickness (MCT) have been considered as reference lines to define different angular metrics and distances: GA–AP, GA–MCT, AP–MCT, anterior AP–MCTd, and posterior AP–MCTd. This kind of analysis may help obtain a better clinical characterization of the level of severity and progression of corneas with keratoconus.

In the current series, we found significantly higher values of the areas of the ACS and PCS of the generated custom 3-D model (A_{ant}, A_{post}) in the groups of eyes with KC, which is consistent with the

results of our previous studies [1–3]. This confirms that the local steepening occurring in the ACS and PCS in KC [5,9,11,12,15,17,31] leads to an increase in the area occupied by each surface. Indeed, the combination of A_{post} and A_{tot} with other morphogeometric parameters has been shown to provide good diagnostic ability for the detection of grade I KC, with sensitivity of 97.4% and specificity of 97.2% [2]. Likewise, significantly lower values of corneal volume were found in the KC group when compared with the control group, which is consistent with the significantly lower pachymetric values obtained. Ahmadi Hosseini et al. [49] demonstrated that the presence of a reduction in corneal volume in keratoconus eyes was related to the lower percentage thickness increase from center to periphery.

Concerning the new morphogeometric parameters, significantly higher values of GA–AP, GA–MCT, and AP–MCT were found in the KC

group compared to the control group. This confirms the loss of the revolution symmetry of the cornea when a KC is present, with more discrepancy in the position of the optic axis (line joining the geometric center of both corneal surfaces) in KC with respect to the line joining the apex points of both corneal surfaces and the line joining the points of the ACS and PCS in the corneal section containing the minimum corneal thickness. This is in line with the results of previous studies that evaluate the changes occurring in the location of the apex of the ACS in KC eyes, with an inferior displacement in most cases [2,11,12]. Furthermore, in our series, statistically significant correlations of GA-AP, GA-MCT and AP-MCT with the severity of the disease graded using the Amsler–Krumeich classification were found, although the strength of these correlations was limited. This shows a trend of the severity of keratoconus to be associated with a progressively more remarked discrepancy between geometric center and anterior and posterior apex and MCT localizations, leading to a more distorted 3-D configuration of the corneal structure, more significant geometric asymmetries in both corneal surfaces and consequently, a poorer optical performance. In agreement with our results, Abu Ameerh and colleagues [12] demonstrated that the vertical apex location in keratoconus was effectively correlated with the level of severity of the disease, but this correlation was weaker for the horizontal location of the apex. Likewise, the asymmetry in pachymetric maps has also been found to be a valuable tool to characterize the structural asymmetry in keratoconus, as well as to provide a consistent detection of the disease [50–52].

In contrast to GA-AP, GA-MCT, and AP-MCT, no clear trends were observed for anterior and posterior AP–MCTd in keratoconus compared to controls. In spite of the significant differences found in the line joining the apex and MCT points of both corneal surfaces, no significant differences in the length of the segment joining the apex and point and minimum corneal thickness on the posterior corneal surface were found between control and keratoconus groups. A small (in magnitude) but statistically significant difference was only found in anterior AP–MCTd between control and keratoconus groups. This confirms that the difference between the apex and MCT point in each surface is less critical than the difference in the projection of these positions on each corneal surface. Therefore, in keratoconus, the correlation between the geometry of both corneal surfaces is altered as has been demonstrated in previous studies [51]. When the correlation of AP–MCTd with the severity grade of the keratoconus was evaluated, a trend toward lower values of anterior and posterior AP–MCTd were found in those eyes with a more severe stage of the disease (negative correlations). This demonstrates that MCT and apex points become closer in both corneal surfaces with an increased level of severity in keratoconus. This is consistent with the results of morphogeometric analyses performed in keratoconus in previous studies of our research group using different parameters, such as the anterior and posterior apex deviations (mean distance from the Z axis to the highest point of both ACS and PCS), and anterior and posterior minimum thickness point deviations (mean distance in the XY plane from the Z axis to the minimum thickness points in both corneal surfaces) [1,2]. However, it should be considered that the correlations found of anterior and posterior AP-MCTd with keratoconus severity grade in our series were limited. Therefore, these parameters may be beneficial to differentiate keratoconus from normal corneas, but possibly are insufficient to be used by clinicians to characterize the level of severity of keratoconus. Future studies should be performed in order to confirm all these trends obtained in the current series.

Finally, we evaluated the correlations between the new morphogeometric parameters and other clinical variables in control and KC groups. In contrast to the lack of significant correlations found in the control groups, several statistically significant correlations of different strength were found in the keratoconus group.

Positive and negative significant correlations of GA–AP and AP–MCT with a great variety of clinical parameters that have been found previously to correlate also with the severity of the disease were found in our keratoconus group [15,17,31,53]. Specifically, poorer CDVA and higher level of coma-like and spherical-like corneal aberrations, as well as more negative asphericity values and lower MCT and CCT, were found in those eyes showing higher values of GA–AP and AP–MCT. This confirms that GA–AP and AP–MCT are parameters with the ability of characterizing the corneal structural changes occurring in keratoconus with an increasing level of severity. Likewise, significant correlations were found between anterior and posterior corneal asphericities and anterior and posterior AP–MCTd. Specifically, higher values of these parameters were found in those eyes with less negative values of asphericity. Therefore, MCT and apex were closer in those eyes with more prolate ACS and PCS, which is associated with the presence of more severe stages of keratoconus [15,17,31,53,54].

This study has some limitations that should be acknowledged. Although the Scheimpflug imaging technology has been shown to provide repeatable geometric and pachymetric measurements in keratoconus eyes [44,45], this consistency of tomographic measurements obtained with this type of technology is poorer than that observed in healthy subjects, especially in terms of posterior corneal shape characterization. Future studies using the same morphogeometric approach but with data obtained using other types of technologies should be performed to confirm these outcomes. Likewise, although the level of interobserver repeatability seems to be low considering that measurements are taken automatically by the device, the observer has an active role and there is a range of acceptable focuses that may lead to variable measurements. For this reason, this factor may be also considered as a potential limitation of the current study and should be addressed in future investigations.

Conclusions

The use of new morphogeometric indices developed considering the position and spatial projection of anterior and posterior corneal apex and MCT points allows a clinical characterization of the 3-D structural alteration occurring in keratoconus. Likewise, this type of analysis may allow the clinician to characterize the level of severity of the disease, with less coincidence in the spatial projection of apex and MCT points of both corneal surfaces, as well as lower separation between these two localizations in each surface in the more advanced stages of keratoconus. These changes, according to the severity of this corneal disease, are consistent with the significant reduction in corneal volume and the significant increase in the area occupied by each corneal surface that is observed. Therefore, besides changes occurring separately in each corneal surface, a significant alteration of the 3-D configuration of the corneal structure is present in keratoconus that should be considered in clinical evaluations and decisions. Future studies should be conducted to evaluate the diagnostic ability of the morphogeometric parameters developed for the detection of subclinical keratoconus, comparing such diagnostic performance with that currently provided by spectral-domain optical coherence tomography.

Conflict of interest

The authors have declared no conflict of interest.

Compliance with Ethics Requirements

All procedures followed were in accordance with the ethical standards of the responsible committee on human experimenta-

tion (institutional and national) and with the Helsinki Declaration of 1975, as revised in 2008 (5). Informed consent was obtained from all patients for being included in the study.

Acknowledgments

Funding

References

[1] Cavas-Martínez F, Fernández-Pacheco DG, De la Cruz-Sánchez E, Martínez JN, Cañavate FJF, Vega-Estrada A, et al. Geometrical custom modeling of human cornea in vivo and its use for the diagnosis of corneal ectasia. PLoS ONE 2014;9 (10):e110249.

[2] Cavas-Martínez F, Bataille L, Fernández-Pacheco DG, Cañavate FJF, Alió JL. A new approach to keratoconus detection based on corneal morphogeometric analysis. PLoS ONE 2017;12(9):e0184569.

[3] Cavas-Martínez F, Bataille L, Fernández-Pacheco DG, Cañavate FJF, Alio JL. Keratoconus detection based on a new corneal volumetric analysis. Sci Rep 2017;7(1):15837.

[4] Martínez-Abad A, Piñero DP, Ruiz-Fortes P, Artola A. Evaluation of the diagnostic ability of vector parameters characterizing the corneal astigmatism and regularity in clinical and subclinical keratoconus. Contact Lens and Anterior Eye. 2017;40(2):88–96.

[5] de Sanctis U, Loiacono C, Richiardi L, Turco D, Mutani B, Grignolo FM. Sensitivity and specificity of posterior corneal elevation measured by Pentacam in discriminating keratoconus/subclinical keratoconus. Ophthalmology 2008;115(9):1534–9.

[6] Ramos-López D, Martínez-Finkelshtein A, Castro-Luna GM, Burguera-Gimenez N, Vega-Estrada A, Pinero D, et al. Screening subclinical keratoconus with placido-based corneal indices. Optom Vis Sci 2013;90(4):335–43.

[7] Kozobolis V, Sideroudi H, Giarmoukakis A, Gkika M, Labiris G. Corneal biomechanical properties and anterior segment parameters in forme fruste keratoconus. Eur J Ophthalmol 2012;22(6):920–30.

[8] Prakash G, Agarwal A, Mazhari AI, Kumar G, Desai P, Kumar DA, et al. A new, pachymetry-based approach for diagnostic cutoffs for normal, suspect and keratoconic cornea. Eye. 2012;26(5):650.

[9] Gordon-Shaag A, Millodot M, Ifrah R, Shneor E. Aberrations and topography in normal, keratoconus-suspect, and keratoconic eyes. Optom Vis Sci 2012;89 (4):411–8.

[10] Touboul D, Bénard A, Mahmoud AM, Gallois A, Colin J, Roberts CJ. Early biomechanical keratoconus pattern measured with an ocular response analyzer: curve analysis. J Cataract Refract Surg 2011;37(12):2144–50.

[11] Wahba SS, Roshdy MM, Elkitkat RS. Naguib KM. Rotating Scheimpflug imaging indices in different grades of keratoconus. Journal of ophthalmology. 2016;2016.

[12] Ameerh MAA, Bussières N, Hamad GI, Al Bdour MD. Topographic characteristics of keratoconus among a sample of Jordanian patients. International journal of ophthalmology. 2014;7(4):714.

[13] Fredriksson A, Behndig A. Measurement centration and zone diameter in anterior, posterior and total corneal astigmatism in keratoconus. Acta Ophthalmol 2017;95(8):826–33.

[14] Hwang ES, Perez-Straziota CE, Kim SW, Santhiago MR, Randleman JB. Distinguishing highly asymmetric keratoconus eyes using combined Scheimpflug and spectral-domain OCT analysis. Ophthalmology 2018;125 (12):1862–71.

[15] Piñero DP, Nieto JC, Lopez-Miguel A. Characterization of corneal structure in keratoconus. Journal of Cataract Refractive Surgery. 2012;38(12):2167–83.

[16] Rabinowitz YS. Keratoconus. Surv Ophthalmol 1998;42(4):297–319.

[17] Alió JL, Piñero DP, Alesón A, Teus MA, Barraquer RI, Murta J, et al. Keratoconus-integrated characterization considering anterior corneal aberrations, internal astigmatism, and corneal biomechanics. Journal of Cataract Refractive Surgery. 2011;37(3):552–68.

[18] Cavas-Martinez F, De la Cruz Sanchez E, Nieto Martinez J, Fernandez Canavate FJ, Fernandez-Pacheco DG. Corneal topography in keratoconus: state of the art. Eye and vision (London, England). 2016;3:5.

[19] Wilson SE, Lin DT, Klyce SD. Corneal topography of keratoconus. Cornea 1991;10(1):2–8.

[20] Piegl L, Tiller W. The NURBS Book: U.S. Government Printing Office; 1997.

[21] Cazón-Martín A, Matey-Muñoz L, Rodríguez-Ferradas MI, Morer-Camo P, González-Zuazo I. Direct digital manufacturing for sports and medical sciences: Three practical cases. Dyna (Spain). 2015;90(6):621–7.

[22] Chakroun F, Colombo V, Lie Sam Foek D, Gallo LM, Feilzer A, Özcan M. Displacement of teeth without and with bonded fixed orthodontic retainers: 3D analysis using triangular target frames and optoelectronic motion tracking device. J Mech Behav Biomed Mater 2018;85:175–80.

[23] Minatel L, Verri FR, Kudo GAH, de Faria Almeida DA, de Souza Batista VE, Lemos CAA, et al. Effect of different types of prosthetic platforms on stress-distribution in dental implant-supported prostheses. Mater Sci Eng, C 2017;71:35–42.

[24] Xu F, Morganti S, Zakerzadeh R, Kamensky D, Auricchio F, Reali A, et al. A framework for designing patient-specific bioprosthetic heart valves using immersogeometric fluid–structure interaction analysis. International Journal for Numerical Methods. Biomed Eng 2018;34(4).

[25] Bataille L, Cavas-Martínez F, Fernández-Pacheco DG, Cañavate FJF, Alio JL. A study for parametric morphogeometric operators to assist the detection of keratoconus. Symmetry 2017;9(12).

[26] Giovanzana S, Kasprzak HT, Pałucki B, Ţălu Ş. Non-rotational aspherical models of the human optical system. J Mod Opt 2013;60(21):1899–905.

[27] Lanchares E, Buey MAD, Cristóbal JA, Calvo B, Ascaso FJ, Malvè M. Computational simulation of scleral buckling surgery for rhegmatogenous retinal detachment: On the effect of the band size on the myopization. Journal of Ophthalmology. 2016;2016..

[28] Robins M, Solomon J, Samei E. Can a 3D task transfer function accurately represent the signal transfer properties of low-contrast lesions in non-linear. CT systems?: SPIE 2018.

[29] Abass A, Vinciguerra R, Lopes BT, Bao F, Vinciguerra P, Ambrosio Jr R, et al. Positions of Ocular Geometrical and Visual Axes in Brazilian, Chinese and Italian Populations. Curr Eye Res. 2018;43(11):1404–14.

[30] Thibos LN, Horner D. Power vector analysis of the optical outcome of refractive surgery. J Cataract Refract Surg 2001;27(1):80–5.

[31] Martínez-Abad A, Piñero DP. New perspectives on the detection and progression of keratoconus. Journal of Cataract Refractive Surgery. 2017;43 (9):1213–27.

[32] Chan TC, Wang YM, Yu M, Jhanji V. Comparison of corneal tomography and a new combined tomographic biomechanical index in subclinical keratoconus. J Refract Surg 2018;34(9):616–21.

[33] Cavas-Martínez F, Fernández-Pacheco DG, Parras D, Cañavate FJ, Bataille L, Alió J. Study and characterization of morphogeometric parameters to assist diagnosis of keratoconus. Biomed Eng Online 2018;17(1):161.

[34] Brunner M, Czanner G, Vinciguerra R, Romano V, Ahmad S, Batterbury M, et al. Improving precision for detecting change in the shape of the cornea in patients with keratoconus. Sci Rep 2018;8(1):12345.

[35] Martínez-Abad A, Piñero DP, Chorro E, Bataille L, Alió JL. Development of a reference model for keratoconus progression prediction based on characterization of the course of nonsurgically treated cases. Cornea 2018;37 (12):1497–505.

[36] Mas-Aixala E, Gispets J, Lupón N, Cardona G. Anterior chamber parameters in early and advanced keratoconus. A meridian by meridian analysis. Contact Lens Anterior Eye. 2018;41(6):538–41.

[37] Gupta N, Trindade BL, Hooshmand J, Chan E. Variation in the best fit sphere radius of curvature as a test to detect keratoconus progression on a Scheimpflug-based corneal tomographer. J Refract Surg 2018;34(4):260–3.

[38] Shajari M, Jaffary I, Herrmann K, Grunwald C, Steinwender G, Mayer WJ, et al. Early tomographic changes in the eyes of patients with keratoconus. J Refract Surg 2018;34(4):254–9.

[39] Shajari M, Steinwender G, Herrmann K, Kubiak KB, Pavlovic I, Plawetzki E, et al. Evaluation of keratoconus progression. Br J Ophthalmol 2019;103(4):551–7.

[40] Bao F, Savini G, Shu B, Zhu S, Gao R, Dang G, et al. Repeatability, Reproducibility, and Agreement of Two Scheimpflug-Placido Anterior Corneal Analyzers for Posterior Corneal Surface Measurement. J Refract Surg 2017;33(8):524–30.

[41] Huang J, Savini G, Hu L, Hoffer KJ, Lu W, Feng Y, et al. Precision of a new Scheimpflug and Placido-disk analyzer in measuring corneal thickness and agreement with ultrasound pachymetry. J Cataract Refract Surg 2013;39 (2):219–24.

[42] Mansoori T, Balakrishna N. Repeatability and agreement of central corneal thickness measurement with non-contact methods: a comparative study. Int Ophthalmol 2017;38(3):959–66.

[43] Montalbán R, Piñero DP, Javaloy J, Alió JL. Intrasubject repeatability of corneal morphology measurements obtained with a new Scheimpflug photography–based system. J Cataract Refract Surg 2012;38(6):971–7.

[44] Montalbán R, Alió JL, Javaloy J, Piñero DP. Intrasubject repeatability in keratoconus-eye measurements obtained with a new Scheimpflug photography-based system. J Cataract Refract Surg 2013;39:211–8.

[45] Savini G, Barboni P, Carbonelli M, Hoffer KJ. Repeatability of automatic measurements by a new Scheimpflug camera combined with Placido topography. J Cataract Refract Surg 2011; 37: 1809-16.

[46] Doğan M, Ertan E. Comparison of central corneal thickness measurements with standard ultrasonic pachymetry and optical devices. Clin Exp Optom 2019; 102: 126-130.

[47] Şimşek A, Bilak Ş, Güler M, Çapkin M, Bilgin B, Reyhan AH. Comparison of Central Corneal Thickness Measurements Obtained by RTVue OCT, Lenstar, Sirius Topography, and Ultrasound Pachymetry in Healthy Subjects. Semin Ophthalmol 2016;31:467–72.

[48] Bayhan HA, Aslan Bayhan S, Can I. Comparison of central corneal thickness measurements with three new optical devices and a standard ultrasonic pachymeter. Int J Ophthalmol 2014;7:302–8.

[49] Hosseini SMA, Mohidin N, Abolbashari F, Mohd-Ali B, Santhirathelagan CT. Corneal thickness and volume in subclinical and clinical keratoconus. Int Ophthalmol 2013;33(2):139–45.

[50] Shetty R, Matalia H, Srivatsa P, Ghosh A. Dupps Jr WJ, Roy AS. A novel Zernike application to differentiate between three-dimensional corneal thickness of normal corneas and corneas with keratoconus. Am J Ophthalmol 2015;160(3). pp. 453–62. e2.

[51] Lim H-B, Tan GS, Lim L, Htoon HM. Comparison of keratometric and pachymetric parameters with Scheimpflug imaging in normal and keratoconic Asian eyes. Clinical ophthalmology. 2014;8:2215.

[52] Akçay S, İlkay B, Özgürhan EB, Bozkurt E, Kurt T, Yıldırım Y, et al. Evaluation of pachymetric measurements with Scheimpflug photography-based system and optical coherence tomography pachymetry at different stages of keratoconus. Journal of Ophthalmology. 2014;2014.

[53] Piñero DP, Alió JL, Alesón A, Vergara ME, Miranda M. Corneal volume, pachymetry, and correlation of anterior and posterior corneal shape in subclinical and different stages of clinical keratoconus. Journal of Cataract Refractive Surgery. 2010;36(5):814–25.

[54] Montalban R, Alio JL, Javaloy J, Pinero DP. Comparative analysis of the relationship between anterior and posterior corneal shape analyzed by Scheimpflug photography in normal and keratoconus eyes. Graefe's archive for clinical and experimental ophthalmology = Albrecht von Graefes Archiv fur klinische und experimentelle. Ophthalmologie 2013;251(6):1547–55.